Pedestal impurity transport with 3D fields in ITER-similar-shape DIII-D plasmas

B.S. Victor[1], T. Odstrcil[2], S.L. Allen[1], C. Chrystal[3], C. Collins[3], B.A. Grierson[4], E. Hinson[5], E.M. Hollmann[6], A. Jarvinen[1], C. Paz-Soldan[3], K.E. Thome[3]

[1] *Lawrence Livermore National Laboratory, Livermore, USA*

[2] *Massachusetts Institute of Technology, Boston, USA*

[3] *General Atomics, San Diego, USA*

[4] *Princeton Plasma Physics Laboratory, Princeton, USA*

[5] *University of Wisconsin, Madison, USA*

[6] *University of California–San Diego, San Diego, USA*

Experiments on DIII-D have shown that resonant magnetic perturbations (RMPs) decrease the perturbative effects of impurities in the H-mode pedestal. STRAHL modeling of discharges with aluminum laser blow off (LBO) injection show increased diffusion in the pedestal of H-mode discharges with RMPs. The increased diffusion prevents the build up of impurities near the edge of the plasma, thereby improving the robustness of the plasma. Tungsten LBO injection into discharges with and without RMPs led to striking differences in the evolution of the discharge. The ELMy discharges without RMPs became ELM free and terminated with a radiative collapse from an increase in edge radiation. Injecting a similar number of particles into discharges with RMPs, either with or without ELMs, led to a measurable accumulation of core W, but did not significantly impact the evolution of the discharge.

Introduction

Impurity transport through the pedestal region of H-mode plasmas is a major factor that will determine the accumulation of W in the core of ITER plasmas. W transport through the H-mode pedestal has been studied on ASDEX Upgrade [1] and JET [2], and extrapolated to ITER [3]. In addition, ITER has 3D field coils for RMP ELM control. Therefore, pedestal impurity transport in some ITER plasmas will be affected by RMPs. These DIII-D experiments were designed to investigate impurity transport in the pedestal region in H-mode plasmas with and without RMPs.

Experiments were performed on DIII-D in H-mode ITER-similar-shape discharges for three cases: 1. ELMy, q_{95} = 3.5, 2. RMP ELM-suppressed, q_{95} = 3.5, and 3. RMP with ELMs, q_{95} = 4.1. These RMPs produce a vacuum perturbation of $\delta B/B \approx 4 \text{ x } 10^{-4}$ in the edge of the plasma. For each of the three cases, W and Al were injected with the laser blow off (LBO) system. LBO injection provides an opportunity to study the initial increase and subsequent relaxation of the impurity density profile as opposed to a continuous and unknown impurity source from the wall or divertor. Four DIII-D diagnostics are used to measure impurity emission in these discharges: charge exchange recombination (CER) spectroscopy [4], a multi-chord

soft x-ray (SXR) system [5], SPRED, and a multi-chord bolometer system. CER measured spatially ($\Delta R \sim 8$ mm) and temporally ($\Delta t \sim 2.5$ ms) resolved emission in the pedestal region of the plasma. Poloidal arrays of SXR chords were used in conjunction with multiple thickness Be filters (125 and 12 μm thick). The CER system has higher spatial resolution and the SXR system has faster temporal resolution. Total radiated power is measured along 48 view chords by a foil bolometer. SPRED provides a measure of the temporal ($\Delta t \sim 2$ ms) evolution of Al emission of select lines between 170 and 1250 $\dot{A}$ in the scrape-off layer.

For discharges with Al injection, these measurements are used in conjunction with the STRAHL transport code [6], interfaced in OMFIT on DIII-D [7], to determine the impurity density and transport coefficients in the pedestal region of the plasma. The STRAHL code incorporates atomic data from ADAS and calculates the temporal and radial impurity transport and emission. Using a plasma equilibrium from EFIT and the temporal evolution of T_e, n_e, and Al emission as inputs, a multi-dimensional minimization is performed to determine the impurity density profile and transport coefficients that best match the experimental measurements. Bayesian sampling of the posterior is done using the EMCEE Markov chain Monte Carlo (MCMC) [8] ensemble sampler, initialized near the maximum likelihood solution, to estimate the uncertainty in the transport coefficients.

Pedestal emission with Al injection

Al was injected into naturally ELMy plasmas, and plasmas with RMPs, with and without ELM suppression. Measurements of the background plasma temperature, density, and radiation indicated that the Al injection was non-perturbative. Using the CER system, local measurements of Al^{13+} emission were made in the pedestal region of the plasma. These measurements, in conjunction with the SXR chords and SPRED spectrometer, constrain the impurity density in the STRAHL calculations. The evolution of $n_{Al^{13+}}$ measured by CER, Fig. 1, shows a large difference between discharges with and without ELMs. The Al^{13+} density from STRAHL tracks the total Al density after the first 50 ms, indicating that $n_{Al^{13+}}$ is a good proxy

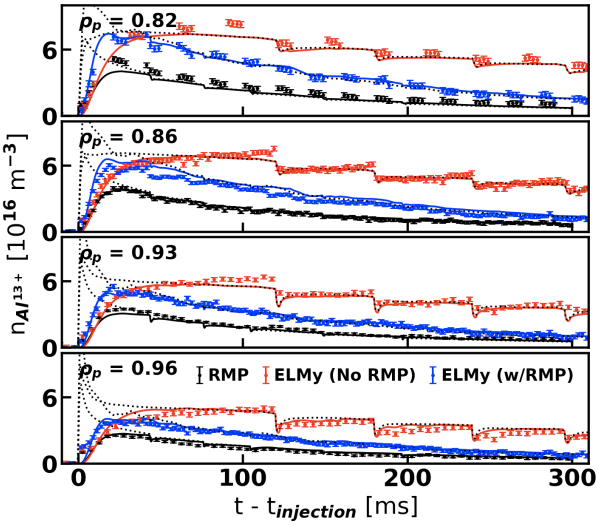

Figure 1: *STRAHL fit (solid lines) compared to CER measurements in the pedestal region for three discharges: RMP ELM suppressed (black, 175674), ELMy without RMPs (red, 175677), and ELMy with RMPs (blue, 175671). Dotted black lines are the normalized total Al density (summation of all Al charge states) from STRAHL.*

for the total Al density. Two sets of transport coefficients are used to model the evolution of the impurity density profile: between (inter) ELMs and during (intra) ELMs. Of note in the pedestal region of the ELMy discharge (red) is that the measured Al^{13+} density increases between ELMs and only decreases during the ELMs. For the discharges with RMPs, there is a continual decrease in the measured Al^{13+} density with or without the presence of ELMs. Difficulty is encountered fitting the evolution of the impurity density in the inter-ELM period. As can be seen in Fig. 1, the STRAHL model does not, in general, show a continual rise in Al^{13+} density in the inter-ELM period. It is challenging to separate scrape-off layer constraints in the minimization process and it takes some level of recycling to match the temporal evolution of the SPRED measurements and the data shown in Fig. 1.

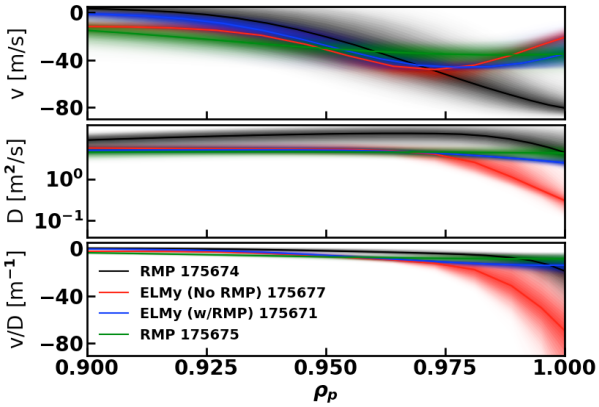

Figure 2: *Transport coefficients found from the STRAHL minimization with Al injection. Confidence levels from Bayesian inference using EMCEE.*

Pinch (v) and diffusion (D) coefficients for the three discharges from Fig. 1, and an additional discharge with RMP ELM suppression, are shown in Fig. 2. Diffusion near the edge of the plasma ($\rho_p > 0.98$) for the ELMy discharge is similar to the diffusion found in Fig. 3 in Ref. [1]. Discharges with RMPs have edge diffusion an order of magnitude larger than discharges without RMPs. The increased diffusion explains the steady decrease in Al density measured in the discharges with RMPs.

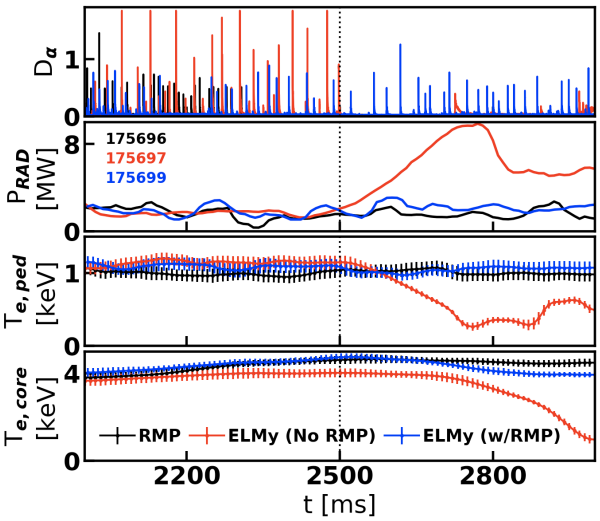

Figure 3: *Discharges with W injection showing a) D_α, b) Total P_{rad} from bolometers, c) pedestal T_e and d) core T_e*

Plasma evolution with W injection

The LBO system injected approximately 4 x 10^{17} W atoms into the three discharge types described above, Fig. 3. After the W injection, the ELMy discharge goes ELM free and experiences a radiative collapse, compared to the discharges with RMPs, which do not experience a significant rise in radiation. W accumulates in the core of the discharges with RMPs, but not at high enough levels to cause a significant

increase in radiation. None of the discharges presented in this paper use ECH power. Future work includes the use of ECH in the RMP discharges to prevent core W accumulation.

Without local W emission measurements in the pedestal, the transport coefficients from the Al discharge provide a guide to understanding the evolution of the discharge without RMPs. Low diffusion near the pedestal leads to an accumulation of W in the pedestal region. This causes radiation to increase, the plasma to go ELM free, and the pedestal temperature to drop, Fig. 3(c). Core temperature does not drop significantly until the pedestal temperature has decrease to 25% of its previous value and total radiation exceeds 8 MW. Thus the plasma is quenched from the outside in.

Summary

Al injection with an LBO system has been used to diagnose impurity transport in the edge of H-mode plasmas with and without RMPs. For the discharges with RMPs, after the initial rise, n_{Al} decreases at a steady rate in the pedestal. However, for the naturally ELMy discharge without RMPs, n_{Al} continues to increase after the initial rise and only decreases during ELMs. STRAHL calculations show that the discharges with RMPs have increased diffusion near the plasma edge, which prevents the build up of impurities in the pedestal. For the case of the naturally ELMy discharge, diffusion near the plasma edge is low during the inter-ELM period and the majority of impurity ejection occurs during ELMs.

W injection into a discharge without RMPs had a more deleterious effect on plasma performance than injection of a similar number of W atoms into a plasma with RMPs. The discharge without RMPs experienced a radiative collapse, with the plasma temperature cooling from the outside in. Discharges with RMPs did not experience a radiative collapse or a decrease in pedestal temperature due to the increased diffusion in the pedestal region from the RMPs.

This work was performed under the auspices of the U.S. Department of Energy by Lawrence Livermore National Laboratory under Contract DE-AC52-07NA27344. This material is based upon work supported by the U.S. Department of Energy, Office of Science, Office of Fusion Energy Sciences, using the DIII-D National Fusion Facility, a DOE Office of Science user facility, under Award DE-FC02-04ER54698.

References

[1] Pütterich T, et al. 2011 *Journal of Nuclear Materials* **415**
[2] Fedorczak N, et al. 2015 *Journal of Nuclear Materials* **463**
[3] Dux R, et al. 2014 *Plasma Physics and Controlled Fusion* **56**
[4] Chrystal C, et al. 2016 *Review of Scientific Instruments* **87**
[5] Hollmann E M, et al. 2011 *Review of Scientific Instruments* **82**
[6] Dux R 2007 Report no. jpp 9/82 Tech. rep. Max Planck Institut fur Plasmaphysik Garching, Germany
[7] Grierson B A, et al. 2015 *Physics of Plasmas* **22**
[8] Foreman-Mackey D, et al. 2013 *arXiv* **125** 306